ORIGINAL PAPER

Geochemical processes analysis and evaluation of groundwater quality in Hamadan Province, Western Iran

Mohammad Nakhaei[1] · Majid Altafi Dadgar[1] · Vahab Amiri[1]

Abstract We attempted to identify the geochemical processes responsible for the present status of groundwater chemistry and to assess the suitability of groundwater for drinking and irrigation purposes in Hamadan province, western Iran. Groundwater from 225 regional deep and dug wells was sampled from eight aquifers and analyzed seasonally during 2013–2014. The major ions (K^+, Na^+, Ca^{2+}, Cl^-, SO_4^{2-}, and HCO_3^-) were used to recognize the hydrochemical characteristics of the groundwater. Results show that the hydrochemistry of Hamadan province is partly due to the weathering process, dissolution of carbonate formations, the cation exchange processes, and chemical inputs from precipitation. The cation dominance order is $Ca^{2+} > Na^+ > Mg^{2+} > K^+$, while the anion dominance order is $SO_4^{2-} > HCO_3^- > Cl^-$. The groundwater type in Hamadan-Bahar, Kabudrahang, and Ghahavand aquifers (central aquifers) is largely characterized as a chloride water type and in the other aquifers (western, southtern, and northern aquifers), relatively shifted to a HCO_3^- water type. Except for a few locations with high values of EC, pH, and other dissolved ions, water quality is suitable for domestic use. Sodium adsorption ratio (SAR), %Na, and permeability index (PI) values suggest suitability of most water samples for irrigation purposes. The majority of water samples belong to C_2S_1 and C_3S_1, indicating medium salinity-low sodium and high salinity-low sodium waters, which high SAR, PI, and Na% in a few locations restricts its suitability for agricultural activities.

Keywords Groundwater quality · Hydrochemical facies · Suitability · Hamadan province

Introduction

Groundwater is the main source of water used for drinking, domestic, industrial, and agricultural purposes in regions where surface water is scarce (Amiri et al. 2015b; Delgado et al. 2010). Groundwater geochemical evolution is controlled by both natural processes and human impacts. Generally in natural systems, geochemical processes of groundwater quality and major components are controlled by natural processes such as mineral weathering, ion exchange, and water-rock interactions, and occurring of these processes is slow (Li et al. 2013a). However, specific hydrogeochemical processes may occur in different hydrogeologic settings. In recharge areas, dissolution of minerals (including carbonates and silicates) dominates (Sung et al. 2012). Precipitation of secondary minerals prevails in discharge areas (Edmunds et al. 2006).

In order to assess hydrogeochemical processes and geochemical evolution in the complex system at basin scale, many methods, including hydrogeochemical diagrams (such as Piper third-line diagrams), multivariate statistical analysis, water-rock interaction simulation, geochemical modeling, and mineral phase equilibrium calculations have been intensively used (Sikdar et al. 2001; Li et al. 2010; Alfy 2012; Li et al. 2013b, c; Wu et al. 2014; Li et al. 2014; Devic et al. 2014; Amiri et al. 2015a), as well as major components, stable isotopes, trace elements, and redox indicators (Barbecot et al.

✉ Majid Altafi Dadgar
Dadgarmajid77@yahoo.com

Mohammad Nakhaei
Nakhaei@khu.ac.ir

Vahab Amiri
Vahab.amiri@gmail.com

[1] Department of Applied Geology, Faculty of Earth Sciences, Kharazmi University, P.O. Box: 31979-37551, Tehran, Iran

2000; Edmunds et al. 2002; Li et al. 2013a, c; Rademacher et al. 2001).

Groundwater is not only the major source of drinking water and agriculture in Iran, especially in semiarid and arid regions, but also supplies more than 50 % of public water utilities and accounts for almost all the water supply to rural households (Mahdavi 2007). In such areas, the quality of groundwater is equally important to its quantity owing to the suitability of water for various purposes (Alaya et al. 2013). Despite the importance of groundwater in Iran, quality assessment of groundwater has received little attention and efforts to use hydrochemical data to solve particular problems are less or nonexistent. Therefore, hydrochemical analysis of the groundwater has become a high priority concern.

This study was carried out in Hamadan province, western Iran. Groundwater is the major source of water for domestic, industrial, and agricultural uses. So far, some researches were reported that in western Iran (e.g., Hamadan province), there exist a variety of environmental problems, such as nitrate contamination and salinization of groundwater (Jalali 2005a, 2007). On the other hand, the studies carried out in this area are focused on some local areas (e.g., Jalali 2009, 2011).

By considering the important role of groundwater in production of agricultural products and drinking purpose, a comprehensive study was needed to evaluate the water chemistry in all aquifers of Hamadan province. Therefore, we attempted to determine the hydrogeochemical nature of the groundwater, identify the geochemical processes responsible for the present status of groundwater quality, and assess the suitability of groundwater for drinking and irrigational uses.

Materials and methods

Study area

Hamadan province with an area of about 19,546 km^2 is situated between longitudes of 47° 45′ E and 49° 29′ E and latitudes of 34° 0′ N and 35° 42′ N, in western Iran (Fig. 1). Hamadan is in the vicinity of the Alvand Mountain and has a cold, mountainous climate, with snowy winters. Hamadan province lies in a temperate mountainous region to the east of Zagros. The vast plains of the north and northeast of the province are influenced by strong winds, which almost last throughout the year. The temperature may drop below −30 °C on the coldest days. The area has a semiarid climate with precipitation during the rainy season, from June to October with a long time average of 234.7 mm per year.

Geological and hydrogeological setting

Based on structural geology, Hamadan province is located at interface between several structural zones. Southwestern

margin of Hamadan province is a portion of high Zagros Mountains, divided from other parts by Borujerd-Morvarid young active faults. Main lithology of this province includes Jurassic-Cretaceous Mountain forming carbonates. The carbonate sheets have been thrusted on each other due to activity of embracing thrusts; therefore, southwestern Hamadan structural characteristics are of thrust faults features. Most parts of Hamadan province belong to northwestern portion of Sanandaj-Sirjan tectono-sedimentary zone which form NW-SE trending heights around Hamadan. These regions are mainly made of metamorphic rocks of two ages: Paleozoic to early Mesozoic and Mesozoic to early Cenozoic. Northeastern parts of Hamadan are plain like regions, which are covered by Quaternary alluvial sediments. Lower cretaceous carbonatic, volcanic rocks specially Oligo-Miocene limestones (Qom formation) outcrops in southern Razan with NW-SE trend.

From hydrogeological points of view, Hamadan province can be divided into eight major aquifers including Asad Abad, Toyserkan, Nahavand, Malayer, Hamadan-Bahar, Razan, Ghahavand, and Kabudrahang. Generally, total groundwater discharge from all aquifers in Hamadan province is about 2381.6 million cubic meters (MCM).

The Asad Abad aquifer extends over an area about 295 km^2. The specific storage in this convertible confined-unconfined aquifer is 0.05. This main lithological unit of this area is limestone formation covering the northern, western, and southern parts. Toward the east and northeast, the aquifer is influenced by the presence of low permeability schist. The thickness of aquifer ranges from 400 m in central part to 20 m in northwest. Groundwater flow down from north and east parts to southern parts of aquifer. The mean annual discharge from this aquifer is about 291.5 MCM per year.

The unconfined Toyserkan aquifer with an area of around 198 km^2, belong to northwestern portion of Sanandaj-Sirjan zone which form NW-SE trend. The specific storage in Toyserkan aquifer is 0.06. Toyserkan aquifer is bounded by limestone units in the south and west. In the northeast and northwest of the aquifer, igneous and metamorphic rocks make the main units. Groundwater flow direction is, in general, from northeast to the southwest. The mean annual discharge from Toyserkan aquifer is about 113.1 MCM.

The unconfined Nahavand aquifer has an area about 644 km^2 is a portion of high Zagros Mountains, divided from other parts by Borujerd-Morvarid young active faults. The specific storage in this aquifer is 0.05. Main lithology of this area includes Jurassic-Cretaceous Mountain forming carbonates and metamorphic rocks. The aquifer has a mean thickness of 100 m and groundwater flow from south to the north. The mean annual groundwater discharge from this aquifer is near 475.2 MCM.

The unconfined Malayer aquifer extends over an area about 520 km^2 and is mainly surrounded by metamorphic (phyllite)
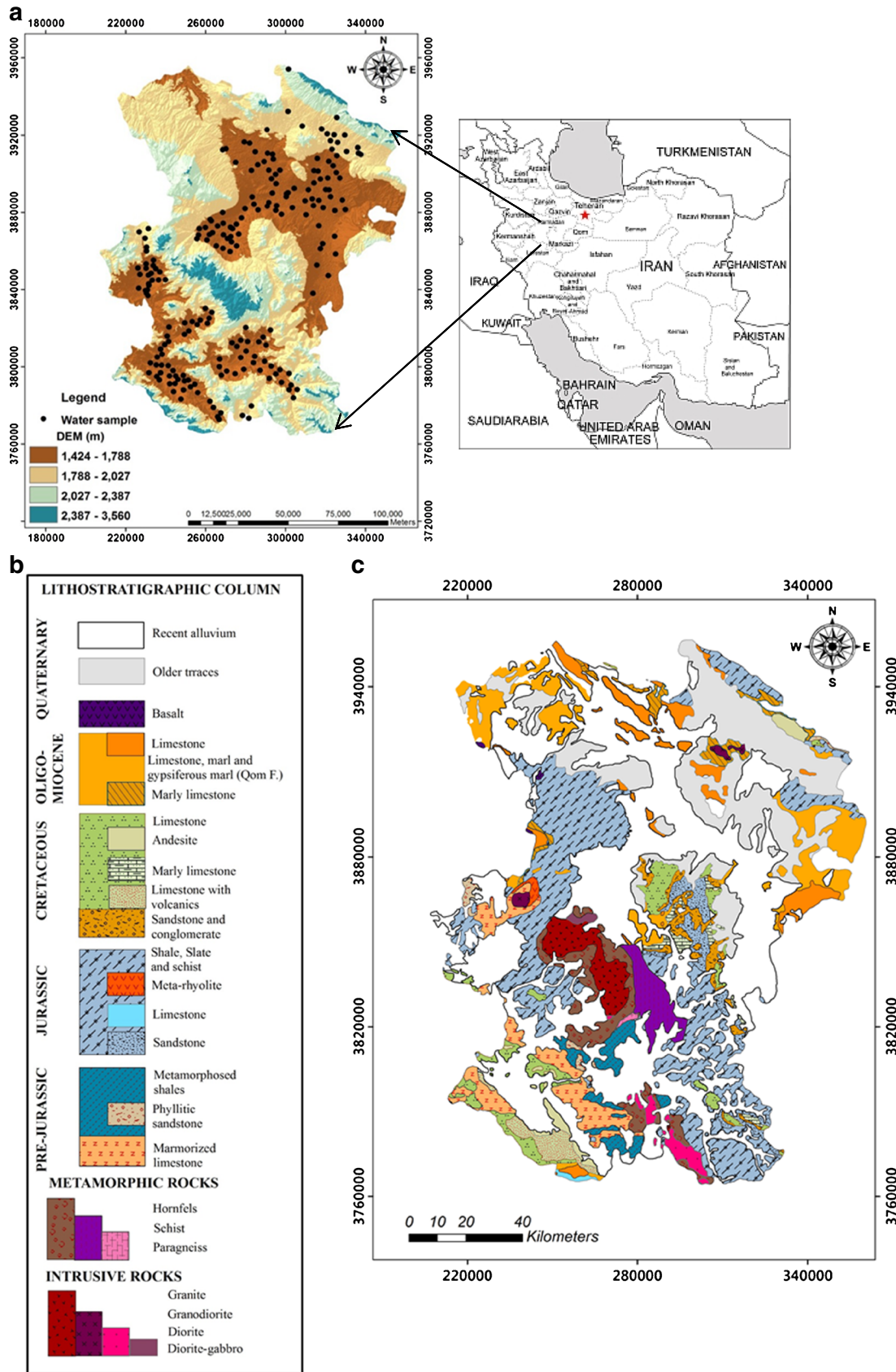
Fig. 1 **a** Digital elevation map and water sample points, **b** geology map, and **c** lithostratigraphic column of Hamadan province

and igneous rocks. The specific storage in this aquifer is 0.04. In this area, limestone unit has a small outcrop in the southeast of the area which form NW-SE trend (Fig. 1a). Groundwater flow direction has a SE-NW trend. The mean annual discharge from this aquifer is about 290.8 MCM.

The unconfined Hamadan-Bahar aquifer with an area of around 468 km^2 and specific storage equal to 0.047 belongs to northwestern portion of Sanandaj-Sirjan tectono-sedimentary zone which form NW-SE trending heights around Hamadan. These regions are mainly made of metamorphic rocks of two ages: Paleozoic to early Mesozoic and Mesozoic to early Cenozoic. Northeastern parts of Hamadan are plain-like regions, which are covered by Quaternary alluvial sediments. Lower cretaceous carbonatic, volcanic rocks specially Oligo-Miocene limestones (Qom formation) outcrops in southern Razan with NW-SE trend. The mean annual groundwater discharge from Hamadan-Bahar aquifer is about 475.2 MCM.

The unconfined Razan and Ghahavand aquifer with an area about 1709 km^2 and is mainly bounded by metamorphic (phyllite), igneous rocks (andesite), Tuff and shale. The specific storage in this aquifer is 0.045. Agriculture is the dominated land use and comprises mostly slope farmland, orchard, field crops, sparse forestland, and residential land. The mean annual discharge from Razan and Ghahavand aquifer is about 486 MCM.

The unconfined Kabudrahang aquifer which has an area about 1350 km^2 and specific storage equal to 0.04 is characterized by the predominance of metamorphic rocks of both sedimentary and magmatic origins. The metamorphic rocks constitute an assemblage of high to low methamorphic grade rocks from sedimentary sequences that have been affected by more- or less-developed tectono-metamorphic events. Basement rocks and minerals in the studied area consist of granites, schist, plagioclase, dolomite, and limestone (Fig. 1c). The mean annual groundwater discharge from this aquifer is near 443 MCM.

Sampling and analyses

In this study, groundwater from 225 regional monitoring wells was sampled from eight aquifers and analyzed seasonally during 2013–2014. The study was conducted for wet and dry seasons separately. In this study, seven chemical parameters including calcium (Ca^{2+}), sodium (Na$^+$), potassium (K$^+$), magnesium (Mg^{2+}), bicarbonate (HCO$_3^-$), sulfate (SO$_4^{2-}$), chloride (Cl$^-$), and four physical parameters including total dissolved solid (TDS), pH (hydrogen ion concentration), TH (Total hardness), and electrical conductivity (EC) were used to evaluate the groundwater quality. The samples were collected after 10 min of pumping and stored in polyethylene bottles. Immediately after sampling, pH, EC, and TDS were measured in the field using a multiparameter portable meter.

Water samples collected in the field were analyzed in the laboratory for cations (Ca^{2+}, Mg^{2+}, Na$^+$, and K$^+$) and anions (HCO$_3^-$, SO$_4^{2-}$, and Cl$^-$) using the standard methods. Ca^{2+} and Mg^{2+} were determined titrimetrically using standard EDTA. Chloride was determined by the standard AgNO$_3$ titration method. Bicarbonate was determined by titration with HCl. Sodium and K$^+$ were measured by flame photometry and SO$_4^{2-}$ by spectrophotometric turbidimetry (APHA 2005).

The quality assurance and quality control (QA/QC) was assured through careful standardization, procedural blank measurement (including field blanks, instrument blank, trip blank, etc.) spiking, and duplicating the samples. The ionic charge balance of each sample was within $\pm \sim 5$ %.

The data were statistically analyzed and a correlation matrix was run using the SPSS 17 software package. The inferential statistics can make judgments of the probability that the difference between groups is a dependable one or independent of each other. The AquaChem 3.7 program was used for hydrochemical assessment of water samples.

The origin and chemical behavior of the groundwater were assessed based on the ionic relationships. These comprise the relationships of TDS vs. Cl$^-$/[Cl$^-$+ HCO$_3^-$], TDS vs. Na$^+$/[Na$^+$+ Ca^{2+}], [Ca^{2+}/Ca^{2+}+Cl$^-$] vs. EC, [Mg^{2+}+ Ca^{2+}] vs. [SO$_4^{2-}$+HCO$_3^-$], [CO$_3^{2-}$+ HCO$_3^-$]-[Cl$^-$+ SO$_4^{2-}$] vs. [Ca^{2+}+ Mg^{2+}]-[Na$^+$+K$^+$] (Chadha diagram), and [Ca^{2+}+Mg^{2+}]-[SO$_4^{2-}$+ HCO$_3^-$] vs. Na-Cl.

The correlations between major cations were studied to clarify which elements contribute to the groundwater composition. In addition, the saturation indices of groundwater samples were calculated using the geochemical model PHREEQC (Parkhurst and Appelo 1999).

The saturation state of the water samples is defined by the saturation index (SI) (Appelo and Postma, 2005) and was calculated based on the activities of free ions in solution. The saturation index (SI) is calculated by comparing the chemical activities of the dissolved ions of the mineral (ion activity product, IAP) with their solubility product (K$_{sp}$). In equation form,

$$SI = \log(IAP/K_{sp}) \tag{1}$$

Some minerals react fast upon contact with water, mostly minerals, such as gypsum, halite, and carbonate, which would meet the equilibrium in a short residence time. SI values equal to 0 indicate equilibrium between the mineral and the solution while positive SI values show supersaturation and negative SI values reflect undersaturation. SI values can be expressed in numerous ways, such as to describe the dissolution or precipitation of minerals (Esmaeili-Vardanjani et al. 2015).

Table 1 Statistical summary of the physical and chemical parameters of groundwater samples in Hamadan province

Parameters	Min.		Max.		Mean		WHO (2004)		WHO (2011)	Samples over max. Permissible limit(%)	
	Wet	Dry	Wet	Dry	Wet	Dry	Most desirable limit	Max. allowable limit	Max. allowable limit	Wet	Dry
K^+ (mg/l)	0.4	0.4	7	7.8	1.2	1.2	–	12	–	0.0	0.0
Na^+ (mg/l)	5.7	4.6	709.2	804.6	84.4	86.2	–	200	200	10.6	11.1
Mg^{2+} (mg/l)	12.1	12.1	200.4	218.7	36.9	38.6	50	150	150	1.8	1.8
Ca^{2+} (mg/l)	36	38	581.1	571.1	89.6	90.9	75	200	200	4.4	5.3
HCO_3^- (mg/l)	164.7	183	1311.5	1226.1	326.7	334.6	–	–	600	–	–
Cl^- (mg/l)	7	7	1125.6	1085.7	65	67.2	200	600	600	0.9	0.8
SO_4^{2-} (mg/l)	4.8	4.8	1862.4	1896	142.6	144.9	200	400	600	8.0	8.5
pH (−)	6.3	6.2	8.2	8	7.5	7.5	6.5	8.5	–	0.0	0.0
TDS (mg/l)	195.2	209.3	4515	4763.7	743	748.4	500	1500	1500	8.0	9.0
EC (µS/cm)	235.5	327	6740	7110	1098.9	1143.4	1400	–	1500	20.0	20.0
TH (mg/l)	145	155	2275	2325	375.8	385.7	–	500	500	13.3	15.5

Results and discussion

Chemical characteristics of water

Minimum, maximum, and mean values of different physical and chemical parameters in groundwater samples collected in wet and dry seasons are given in Table 1. The mean concentrations of Ca^{2+} in the wet and dry seasons are 89.62 and 90.90 mg/l, respectively, which are presumably derived from calcium-rich minerals (e.g., carbonate minerals). As shown in Fig. 1c, limestone formations are distributed almost throughout the study area. The mean concentrations of Na^+ and K^+ in groundwater are 84.43 and 86.26 mg/l, and 1.23 and 1.24 mg/l for wet and dry seasons, respectively. Based on variety of rock formations (i.e., volcanic, metamorphic and sedimentary) in this area and role of water-rock interaction in the change of water chemistry (Fig. 2), the major source of Mg^{2+} in the groundwater may be due to dissolution of Mg-bearing rocks

(e.g., dolomitic formations). The average concentrations of Mg^{2+} and HCO_3^- ions found in the groundwater samples in the study area are 36.97 and 38.61 mg/l, and 326.74 and 334.63 mg/l for wet and dry seasons, respectively. The average values of sulfate in the wet and dry seasons are 142.65 and 144.96 mg/l, respectively. The concentration of Cl^- ranges from 7.03 to 1125.60 and 7.03 to 1085.73 mg/l in the wet and dry seasons, respectively. In the wet season, pH values vary from 6.25 to 8.25, while in the dry season, it varies from 6.20 to 8.0. This indicates that most groundwater samples have alkaline nature. The sampling sites with slightly acidic water (pH < 7) are located in the east of study area (Ghahavand aquifer). The most important economic activity of the area is agriculture. Therefore, anthropogenic pollution such as oxidation of ammonium originated from fertilizers can lead to increase in water acidity. The EC values vary from 235.5 to 6740 µS/cm in wet season and from 327 to 7110 µS/cm in dry season (Table 1). In this region, cation
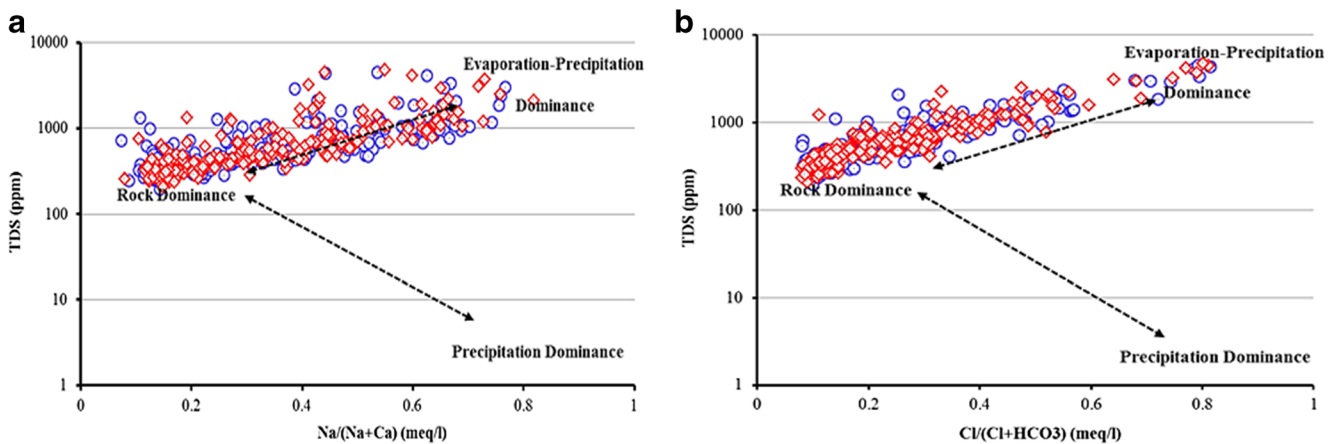

Fig. 2 Mechanisms governing groundwater chemistry **a** TDS vs. $Na^+/[Na^+ + Ca^{2+}]$, **b** TDS vs. $Cl^-/[Cl^- + HCO_3^-]$ (*circle* = wet season; *diamond* = dry season)

dominance order is $Ca^{2+} > Na^+ > Mg^{2+} > K^+$, while the anion dominance order is $SO_4^{2-} > HCO_3^- > Cl^-$. No seasonal variation was noticed in the ionic dominance pattern.

Pearson correlation analysis is a useful tool in hydrogeochemical studies since the produced correlation matrix can indicate associations between individual parameters, thus demonstrating the overall coherence of the data set and revealing the links between individual variables and various controlling factors (Wang and Jiao 2012).

If the correlation coefficient (r) is greater than 0.7, two parameters are considered to be strongly correlated, whereas if the r value is between 0.5 and 0.7, it indicates a moderate correlation at a significance level $p < 0.05$ (Guey-Shin et al. 2011). In the present study, the statistical software package SPSS 17.0 for Windows was used to calculate Pearson correlation coefficients, with the obtained results listed in Table 2 (bottom and top triangles indicating wet and dry, respectively). As seen from Table 2, all major cations and anions with the exception of HCO_3^- have a strong correlation ($r > 0.9$) with TDS. Calcium and Mg^{2+} presented a positive correlation ($r = 0.96$), indicating a common source (limestone, dolomite, and metamorphose carbonate rocks). Correlation between Ca^{2+} and

HCO_3^- (slightly weak) in comparison with correlation between Ca^{2+} and SO_4^{2-} (strong) shows the latter ions in groundwater are mainly provided by the dissolution of gypsum. There is a strong correlation between Na^+ and Cl^-, indicating that dissolution of chloride salts (Qom formation) can be referred as the main source of salinity, because the groundwater level descend to a minimum depth of about 10 m. So, evaporation is not the main reconcentration process. EC exhibits an excellent correlation with TDS ($r = 0.99$) during wet and dry seasons. This occurs because TDS depends on dissolved ion concentration. Groundwater chemistry depends on a number of factors, such as general geology, degree of chemical weathering of the various rock types, quality of recharge water, and inputs from sources other than water-rock interaction (Sarath Prasanth et al. 2012).

The functional sources of dissolved ions can be broadly assessed by plotting the samples, according to the variation in the ratio of $Na^+/[Na^++Ca^{2+}]$ and $Cl^-/[Cl^-+HCO_3^-]$ as a function of TDS (Gibbs 1970). A Gibbs plot (Fig. 2a, b) of data indicates that groundwater chemistry in this area may have been mainly governed by rock weathering. However, rock-weathered materials

Table 2 Pearson correlation coefficients of hydrochemical indices (a) wet season and (b) dry season

(a)

Parameters	K^+	Na^+	Mg^{2+}	Ca^{2+}	HCO_3^-	Cl^-	SO_4^{2-}	pH	TDS	EC	TH
K^+	1										
Na^+	0.89	1									
Mg^{2+}	0.89	0.81	1								
Ca^{2+}	0.82	0.76	0.94	1							
HCO_3^-	0.54	0.48	0.6	0.59	1						
Cl^-	0.78	0.82	0.86	0.9	0.49	1					
SO_4^{2-}	0.84	0.87	0.78	0.69	0.25	0.6	1				
pH	−0.42	−0.35	−0.51	−0.56	−0.71	−0.47	−0.19	1			
TDS	0.91	0.94	0.94	0.92	0.57	0.9	0.84	−0.49	1		
EC	0.92	0.94	0.94	0.92	0.57	0.9	0.85	−0.47	0.99	1	
TH	0.86	0.79	0.98	0.99	0.6	0.9	0.74	−0.55	0.94	0.94	1

(b)

Parameters	K^+	Na^+	Mg^{2+}	Ca^{2+}	HCO_3^-	Cl^-	SO_4^{2-}	pH	TDS	EC	TH
K^+	1										
Na^+	0.89	1									
Mg^{2+}	0.93	0.81	1								
Ca^{2+}	0.9	0.76	0.96	1							
HCO_3^-	0.54	0.52	0.62	0.6	1						
Cl^-	0.9	0.83	0.89	0.91	0.52	1					
SO_4^{2-}	0.84	0.88	0.81	0.75	0.32	0.67	1				
pH	−0.48	−0.39	−0.56	−0.6	−0.73	−0.52	−0.26	1			
TDS	0.96	0.94	0.95	0.92	0.59	0.92	0.88	−0.51	1		
EC	0.96	0.94	0.95	0.93	0.61	0.92	0.88	−0.52	0.99	1	
TH	0.92	0.79	0.98	0.99	0.61	0.91	0.78	−0.59	0.94	0.94	1

derived from the underlying rocks control the groundwater chemistry of water samples.

From Fig. 2a, some of samples fell near the evaporation-precipitation zone. As it mentioned in previous section, depth to groundwater level in all aquifers is more than 10 m and groundwater is almost impossible to evaporate. But in the past, groundwater depth might be small and evaporation had significant influences on groundwater chemistry (Fig. 2b). It should be noted that some areas are covered by evaporite and quite soluble sediments such as gypsum (Qom formation). Therefore, like the evaporation process, dissolution of such sediments may remain the similar changes on groundwater chemistry.

For further classification of the analyzed waters, we set a van Wirdum's diagram (van Wirdum 1980), the ionic ratio (IR) vs. the in meq/l (Fig. 3).

$$IR = [Ca^{2+}]/[Ca^{2+} + Cl^-] \qquad (2)$$

The EC can be seen as a measure of the salinity, the IR as a measure of the prevalence of calcium among the cations and chloride among the anions. This prevalence is a result of geochemical processes that occurred within the aquifer. Based on the position in the van Wirdum's diagram, the groundwater can be classified as atmospheric, At (rainwater); lithotrophic, Li (calcium-rich freshwater); thalassotrophic, Th (seawater); or anything in between. The most of samples are distributed around the lithotrophic water type. However, a few of the samples from the Ghahavad aquifer have higher chloride content. As it can be seen in Fig. 3, location of samples plotted near Th zone, both of dry and wet samples have the same location and the sources of salinity cannot be from evaporation, because in wet season in area with cold climate, evaporation from water table is negligible. However, the main sources of salinity provided by dissolution of saline sediments (Qom formation) around the Ghahavand aquifer.
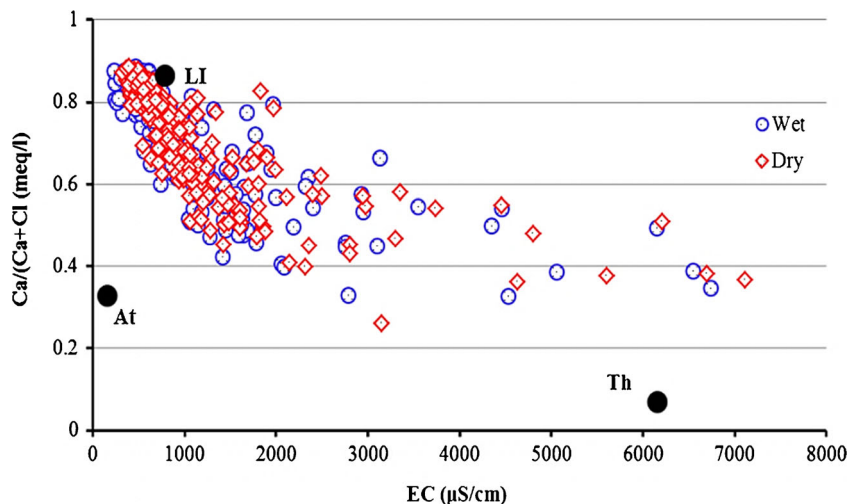
Hydrochemical facies

Groundwater samples of the study area have been plotted on Chadha's diagram (1999). In this scheme, the difference in milliequivalent (epm) percent between alkaline earth (calcium + magnesium) expressed as percentage reacting value is plotted on the x-axis and the difference in milliequivalent (epm) percentage between weak acid anions (carbonate + bicarbonate) and strong acid anions (chloride, sulfate, and nitrate) is plotted on the y-axis.

The milliequivalent percentage difference between alkaline earth and alkalies and between weak acidic anions and strong acidic anions is plotted on one of the four possible subfields of the diagram. In both wet and dry seasons 80 % samples are Ca-Mg-HCO$_3$ type, 13.72 % samples are Ca-Mg-Cl-SO$_4$ type, and 7.84 % samples are Na-K-Cl-SO$_4$ (Fig. 4).

In general, there are three dominant facies, including sulfate, bicarbonate, and chloride. Using results of AquaChem program, the spatial distribution of general water types in the study area have been shown in Fig. 5. This figure generally shows that Hamadan-Bahar, Kabudrahang, and Ghahavand aquifers (central aquifers) have chloride water type and other aquifers (west, south, and northern aquifers) have bicarbonate water type.

Saturation indices

The saturation index (SI) values of minerals were calculated using the PHREEQC software to evaluate the degree of equilibrium between water and the respective mineral and to understand the geochemical processes governing hydrochemistry of groundwater in the area. Figure 6 shows SI indices of water samples relative to anhydrite, aragonite, calcite, dolomite, and gypsum. As it shows, groundwater samples are under saturation relative to anhydrite and gypsum (SI < 0) and it can be expected that negative SI values can

Fig. 3 The van Wirdum's diagram for Hamadan groundwater samples (*At* atmospheric, *Li* lithotrophic, *Th* thalassotrophic groundwater)

Fig. 4 Classification of groundwater samples on Chadha's scheme (circle = wet season; diamond = dry season)
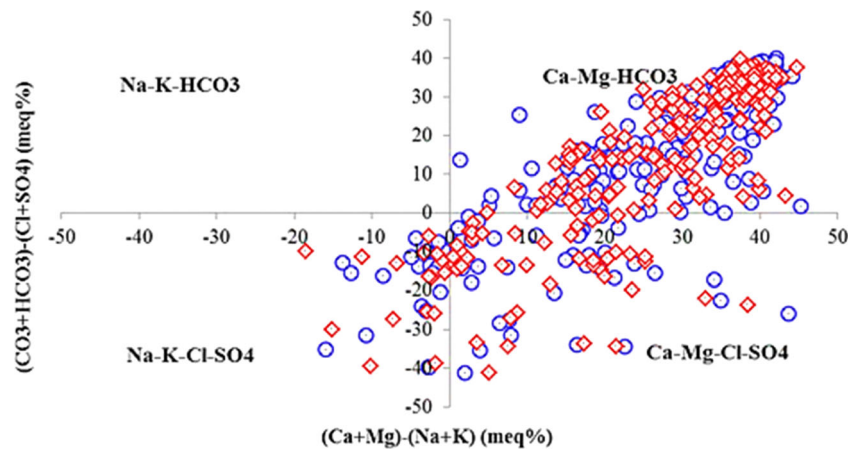
increase the potential of sulfate compositions dissolution (e.g., anhydrite and gypsum) and lead to an increase in concentration of calcium and sulfate ions along groundwater flow direction. So, it should be expected that the water type change from bicarbonate to sulfate (Amiri et al. 2014). The SI values relative to aragonite, calcite, and dolomite are increasingly supersaturated (SI > 0). It is compatible with the origin of groundwater from limestone and dolomite formations which make highland areas through the study domain. No seasonal variation was noticed in the ionic dominance pattern.

Ion exchange reactions

Another significant factor affecting the constituents of groundwater is ion exchange which has become an important

topic for hydrogeologists since it regulates the transport of pollutant chemicals in both aquifers and soils (Appelo and Postma 2005). Ion exchange involves the replacement of ions adsorbed on the surface of the fine-grained materials of the aquifers by ions that are in the solutions (Kazemi and Mohammadi 2012).

Ion exchange and industrial and/or agricultural contamination are likely responsible for increase in sodium in a gneissic terrain (Guo and Wang 2004). High concentration of Na^+ with respect to Cl^- or depletion of Na^+ with respect to Cl^- is the evidence of cation exchange reactions (Salama 1993; Rajmohan and Elango 2004). In the normal ion exchange reaction, Ca^{2+} is retained in the aquifer material and Na^+ is released to water. The excess Na^+ generated by ion exchange reaction is not balanced by Cl^- but by alkalinity or SO_4^{2-}.
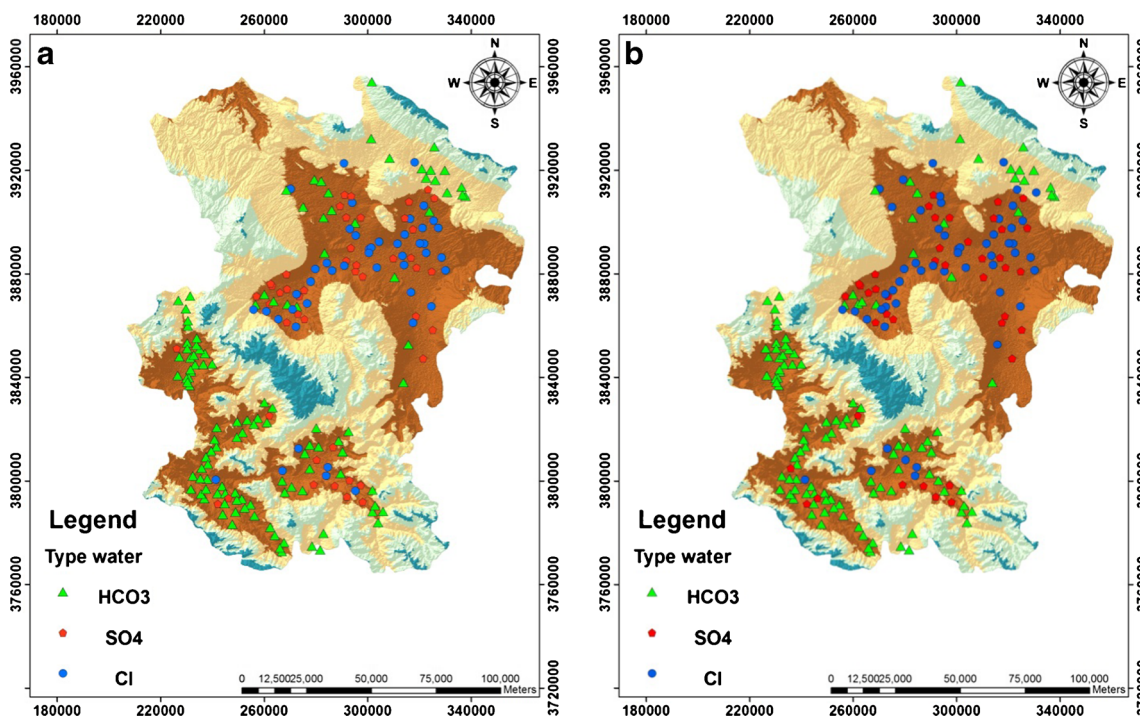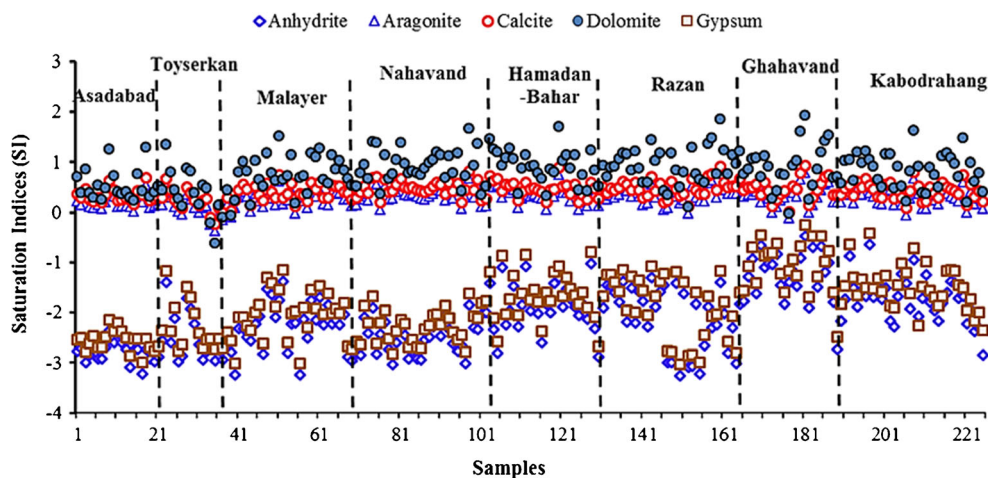

Fig. 5 Map showing water types in the study area (**a** wet season, **b** dry season)

Fig. 6 Saturation indices of minerals related to groundwater samples

Similarly, in the reverse ion exchange, Na^+ is retained by aquifer materials and Ca^{2+} is released to water.

To investigate the importance of ion-exchange processes in groundwater chemistry, we have examined the relationship between the concentration of (Na^+-Cl^-) against $(Ca^{2+}+Mg^{2+}-SO_4^{2-}-HCO_3^-)$ (Fig. 7a). The product of (Na^+-Cl^-) represents excess sodium, that is, sodium coming from the sources other than halite dissolution, assuming that all chloride is derived from halite.

Also, the product of $(Ca^{2+}+Mg^{2+}-SO_4^{2-}-HCO_3^-)$ represents the calcium and/or magnesium coming from sources other than gypsum and carbonate dissolution. In the absence of these reactions, all data should plot close to the origin (McLean et al. 2000). If these processes are significant composition governing processes, the relation between these two parameters should be linear with a slope of −1. As shown, almost all data plot for both wet and dry seasons have a linear correlation, with a slope of about −0.99 for wet and dry seasons. Figure 7 b shows the amount of $Ca^{2+}+Mg^{2+}$ gained or lost relative to that provided by calcite, dolomite, and gypsum. When $HCO_3^-+SO_4^{2-}$ is low (less than 5 meq/l) and the samples plot on 1:1 line, dissolution of calcite and dolomite is the

major process influencing water chemistry but when $HCO_3^-+SO_4^{2-}$ is more than 5 meq/l, in addition to calcite and dolomite, dissolution of gypsum is also likely (Kalantary et al. 2007). For all samples of the Hamadan province, $HCO_3^-+SO_4^{2-}$ is >5 meq/l, indicating that gypsum dissolution is likely to occur. The plot for $Ca^{2+}+Mg^{2+}$ versus $SO_4^{2-}+HCO_3^-$ is another major indicator to identify ion exchange process activated in the study area. If ion exchange is the process, the points shift to the right side of the plot due to excess $SO_4^{2-}+HCO_3^-$. If reverse ion exchange is the process, points shift left due to excess $Ca^{2+}+Mg^{2+}$. The plot of the $Ca^{2+}+Mg^{2+}$ versus $SO_4^{2-}+HCO_3^-$ (Fig. 7b) shows that most of groundwater samples in study area, are located around and below the 1:1 line, indicating ion exchange.

Evaluation of groundwater quality

Suitability for drinking and domestic purposes

According to Table 1, the average values of individual parameters of groundwater are within the permissible limits recommended by WHO (2004, 2011) whereas some samples show
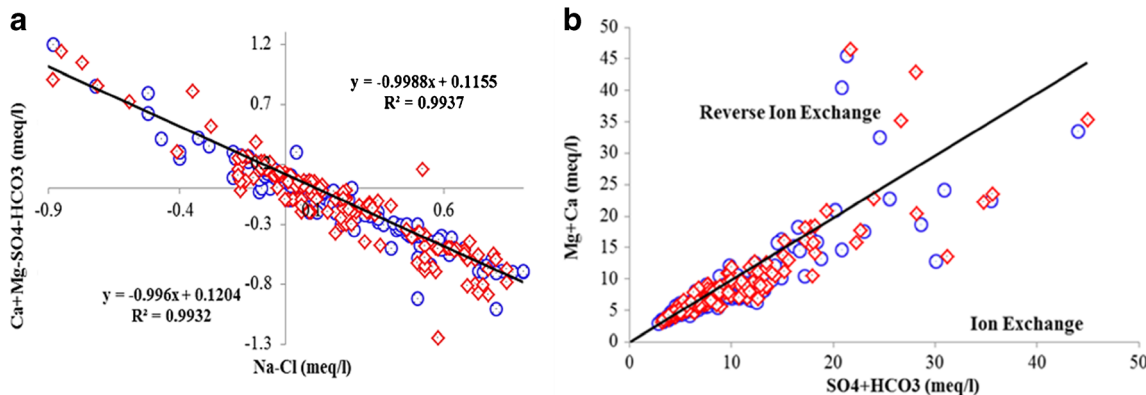

Fig. 7 Plot of **a** $(Ca^{2+}+Mg^{2+})-(SO_4^{2-}+HCO_3^-)$ versus $(Na^++K^+)-Cl^-$ and **b** $Mg^{2+}+Ca^{2+}$ versus $SO_4^{2-}+HCO_3^-$ (*diamond* = wet season; *circle* = dry season)

higher values than permissible limits. Incorporated groundwater suitability map for drinking purposes in the study area is created by combining all the quality parameters, e.g., TDS, TH, pH, Na^+, K^+, Ca^{2+}, Mg^{2+}, Cl^-, and SO_4^{2-} (Fig. 8a, b). For preparing this map, a condition was defined for every sample based on three limitations recommended by WHO (2004, 2011), including most desirable limit, maximum allowable limit, and unsuitable. The condition defined so that if every

quality parameter in every sample exceeds cutoff value of each group, the sample will be categorized in most desirable limit, maximum allowable limit, and unsuitable groups, respectively. For example, if $Cl^-≤200$ mg/l, and the same for all parameters, sample locates in most desirable limit group; if $Cl^->600$ mg/l, sample locates in unsuitable group; and if $200 < Cl^-≤600$, sample locates in maximum allowable limit group. Based on Fig. 8a, b, eight samples of wet season and
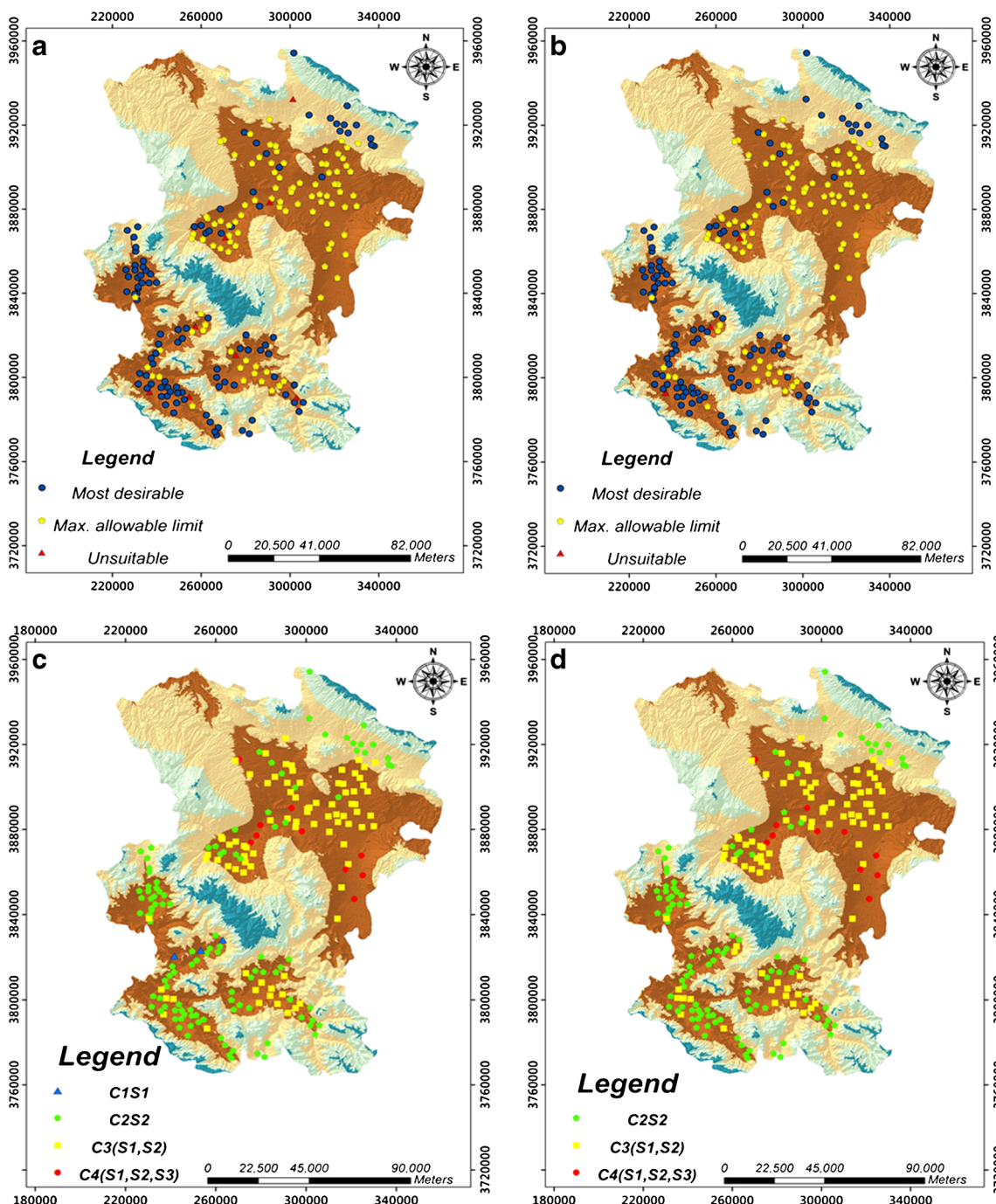

Fig. 8 Groundwater suitability map (a wet and b dry) for drinking in the study region based on WHO (2004, 2011). Groundwater quality map (c wet and d dry) for irrigation based on US salinity hazard diagram samples

three samples of dry season lie in unsuitable quality for drinking. In comparison with geology map (Fig. 1c), it can be referred that these samples are around the metamorphic rocks.

Irrigation suitability

In this region, groundwater is extensively used for irrigation. Therefore, the water suitability for irrigational purposes was assessed using sodium percentage (Na%), sodium adsorption ratio (SAR), and permeability index (PI).

Sodium percent

In all natural waters, sodium percentage (Na%) is a common parameter used to assess its suitability for agricultural purposes (Wilcox 1958).

A high sodium percent causes de-flocculation and impairment of the tilth and permeability of soils (Karanth 1987). The sodium percentage (Na%) in the groundwater is calculated by the following equation:

$$Na\% = Na + K/(Ca + Mg + Na + K) \times 100 \qquad (3)$$

where the quantities of Ca^{2+}, Mg^{2+}, Na^+, and K^+ are expressed in meq/l. Wilcox diagram shows that 4.5 % of the groundwater samples fall in the field of unsuitable, 4.9 % of

the samples fall in the doubtful to unsuitable field, 2.5 % of the samples fall in the field of permissible to doubtful field, and the rest fall in the field of very good and permissible to good (Fig. 9a).

Sodium adsorption ratio

The sodium or alkali hazard in the use of water for irrigation is determined by the absolute and relative concentration of cations and is expressed in terms of SAR. SAR is a measure of the suitability of water for use in agricultural irrigation, because sodium concentration can reduce the soil permeability and soil structure (Todd 1980), the following equation:

$$SAR = Na/[(Ca + Mg)/2]^{0.5} \qquad (4)$$

where sodium, calcium, and magnesium are in meq/l. Excessive sodium content relative to the calcium and magnesium may deteriorate the soil characteristics, thereby reducing the soil permeability and inhibiting the supply of water needed for the crops. The SAR is used to predict the sodium hazard of high carbonate waters, especially if they contain no residual alkali. There is a significant relationship between SAR values of irrigation water and the extent to which sodium is adsorbed by the soils. If water used for irrigation is high in sodium and
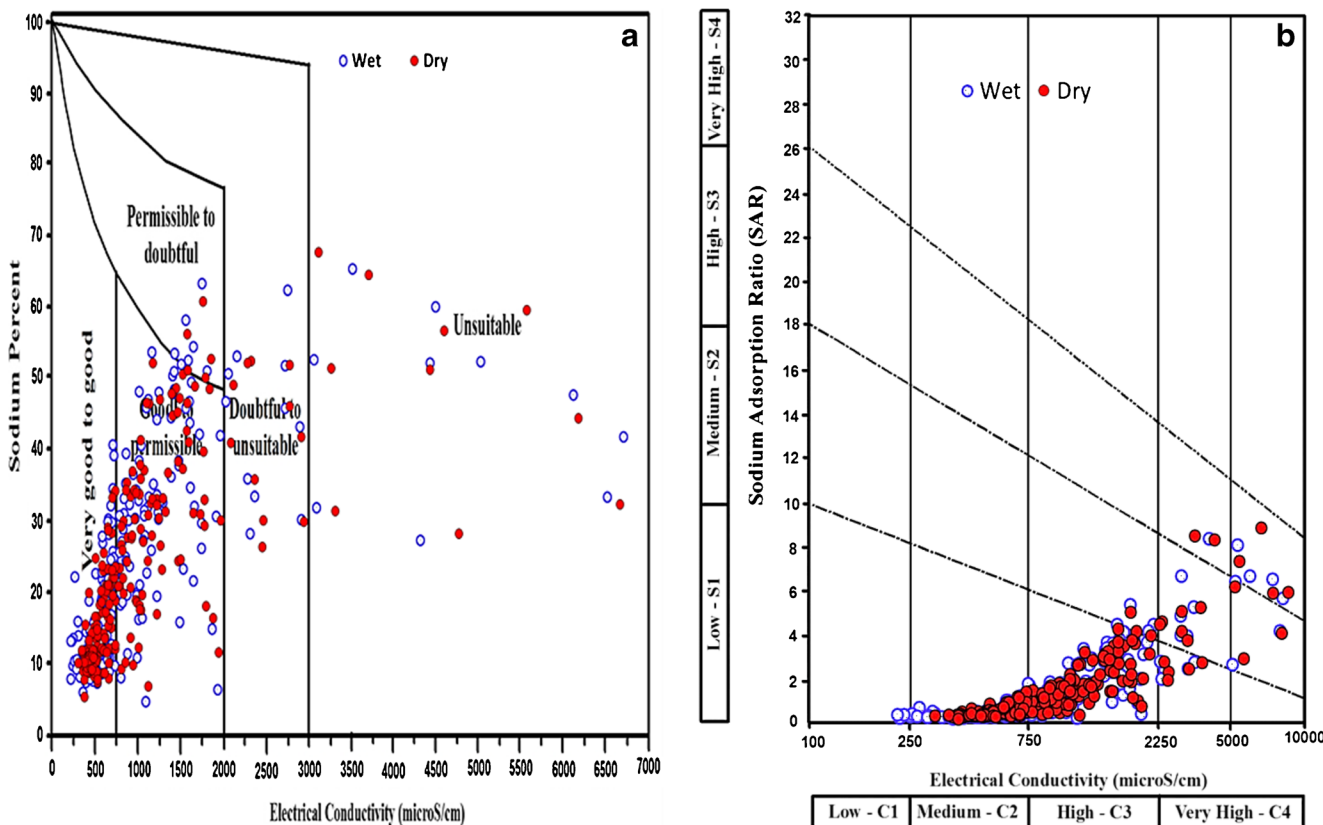

Fig. 9 **a** Classification of irrigation water quality, with respect to total salt concentration and sodium percent and **b** US salinity hazard diagram samples (after Richards 1954).

low in calcium, the cation-exchange complex may become saturated with sodium. This can destroy the soil structure due to the dispersion of clay particles. On the basis of US Salinity Laboratory, hazard diagram (Fig. 9b) can be plotted by correlating the sodium absorption ratio and electrical conductivity (Richards 1954). Water classes of most of the water samples are C_2-S_1, C_3-S_1, indicating medium to high salinity and low sodium type, and about 6.5 % of the samples are C_4-S_2 and C_4-S_3 classes, indicating high to very high salinity and medium to high sodium type. This type of water can be used to irrigate salt tolerant and semitolerant crops under favorable drainage condition. In general, Fig. 9b indicates that the water type in the study area has medium salinity with low sodium content (with the exception of some samples in Ghahavand aquifer which have high sodium content) and it can be used for irrigation on all type of soil. Also, like drinking maps, based on US Salinity Laboratory hazard diagram, a condition was defined so that samples can be categorized in four groups which, including C_1S_1, C_2S_2, $C_3(S_1,S_2)$, and $C_4(S_1,S_2,S_3)$. Figure 8b, c shows the groundwater suitability maps for irrigation. As it can be found, some samples in Ghahavand and Hamadan aquifers lie in $C_4(S_1, S_2, S_3)$ which are near the saline sediments of Qom formation. The solution of halite is the main source of salinity in these samples.

Permeability index

Doneen (1962) evolved a criterion for evaluating the suitability of water for irrigation based on PI. This is calculated using the following equation:

$$PI = \left[(Na + (HCO_3))^{0.5}/(Ca + Mg + Na) \right] \times 100 \qquad (5)$$

Here, all the values are in meq/l. The PI values >75 indicate the excellent quality of water for irrigation. The PI values between 25 and 75 indicate good quality of water and <25 is unsatisfactory for irrigation (Saleh Al-Amry 2008). Collected samples in this area have PI ranged from 22 to 79 %. With respect to PI values, about 96 % of the groundwater samples in the study area can be designated as class II (25–75 %) implying that the water is good quality for irrigation purposes.

Conclusion

Groundwater chemistry in Hamadan province (including eight aquifers), west of Iran, was analyzed to classify the water samples into different categories for drinking and irrigation purposes. The variations of major ions (K^+, Na^+, Ca^{2+}, Cl^-, SO_4^{2-}, and HCO_3^-) was used to recognize the hydrochemical characteristics of the groundwater resources. Based on this study, groundwater chemistry is mainly influenced by rock weathering (water-rock interaction). The cation dominance

order is $Ca^{2+} > Na^+ > Mg^{2+} > K^+$, while the anion dominance order follows $SO_4^{2-} > HCO_3^- > Cl^-$. The hydrogeological interactions between static and dynamic components of aquifer such as rock formations and groundwater flow, respectively, can determine the groundwater quantity and quality. The groundwater type is largely characterized as a chloride water type in Hamadan-Bahar, Kabudrahang, and Ghahavand aquifers (central aquifers) which are around the saline sediment of Qom formation, and relatively shifted to a HCO_3^- water type in the other aquifers (western, southern, and northern aquifers) which locate near the carbonate sediment and metamorphic rocks. The predominance of Na^+ ions in the groundwater is mostly from the cation exchange process, which can be supported from the ionic ratio calculation ((Na^+-Cl^-) against ($Ca^{2+} + Mg^{2+}$-$SO_4^{2-}HCO_3^-$) and ($SO_4^2 + HCO_3^-$) vs. ($Ca^{2+} + Mg^{2+}$)). These observations have major consequences with respect to SI determination which it shows, groundwater samples are under saturation relative to anhydrite and gypsum (SI < 0) and relative to aragonite, calcite, and dolomite are increasingly supersaturated (SI > 0). Groundwater of this area is suitable for domestic purposes except for a few locations where high EC, pH, and other dissolved ions make it unsafe for drinking. SAR, Na%, and PI values suggest suitability of most water samples for irrigation purposes. The majority of water samples belong to C_2S_1 and C_3S_1, indicating medium salinity-low sodium water and high salinity-low sodium, which high SAR, PI, and Na% in few locations restricts its suitability for agricultural activities.

References

Alaya MB, Saidi S, Zemni T, Zargouni F (2013) Suitability assessment of deep groundwater for drinking and irrigation use in the Djeffara aquifers (Northern Gabes, south-eastern Tunisia). Environ Earth Sci. doi:10.1007/s12665-013-2729-9

Alfy ME (2012) Integrated geostatistics and GIS techniques for assessing groundwater contamination in Al Arish area, Sinai, Egypt. Arab J Geosci 5:197–215. doi:10.1007/s12517010-0153-y

Amiri V, Nakhaei M, Lak R, Kholghi M (2015a) Assessment of seasonal groundwater quality and potential saltwater intrusion: a study case in Urmia coastal aquifer (NW Iran) using the groundwater quality index (GQI) and hydrochemical facies evolution diagram (HFE-D). Stoch Env Res Risk A. doi:10.1007/s00477-015-1108-3

Amiri V, Rezaei M, Sohrabi N (2014) Groundwater quality assessment using entropy weighted water quality index (EWQI) in Lenjanat, Iran. Environ Earth Sci 72:3479–3490

Amiri V, Sohrabi N, Altafi Dadgar M (2015b) Evaluation of groundwater chemistry and its suitability for drinking and agricultural uses in the Lenjanat plain, central Iran. Environ Earth Sci 74:6163–6176

APHA (2005) Standard methods for the examination of water and waste-water (21st edition). American Public Health Association, Washington

Appelo CAJ, Postma D (2005) Geochemistry, groundwater and pollution, 2nd edn. Balkema, Rotterdam

Barbecot F, Marlin C, Gibert E, Dever L (2000) Hydrochemical and isotopic characterization of the Bathonian and Bajocian coastal aquifer of the Caen area (northern France). Appl Geochem 15:791–805

Chadha DK (1999) A proposed new diagram for geochemical classification of natural water and interpretation of chemical data. Hydrogeol J 7:431–439

Delgado C, Pacheco J, Cabrera A, Batllori E, Orellana R, Bautista F (2010) Quality of groundwater for irrigation in tropical karst environment: the case of Yucata'n, Mexico. Agric Water Manag 97: 1423–1433. doi:10.1016/j.agwat

Devic G, Djordjevic D, Sakan S (2014) Natural and anthropogenic factors affecting the groundwater quality in Serbia. Sci Total Environ 468-469:933–942

Doneen LD (1962) The influence of crop and soil on percolating water. Proc. 1961 Biennial conference on Groundwater Recharge, 156–163.

Edmunds WM, Carrillo-Rivera JJ, Cardona A (2002) Geochemical evolution of groundwater beneath Mexico City. J Hydrol 258:1–24

Edmunds WM, Ma JZ, Aeschbach-Hertig W, Kipfer R, Darbyshire DPF (2006) Groundwater recharge history and hydrogeochemical evolution in the Minqin Basin, North West China. Appl Geochem 21:2148–2170

Esmaeili-Vardanjani M, Rasa I, Amiri V, Yazdi M, Pazand K (2015) Evaluation of groundwater quality and assessment of scaling potential and corrosiveness of water samples in kadkan aquifer, Khorasan-e-Razavi Province, Iran. Environ Monit Assess 187:53. doi:10.1007/s10661-014-4261-0

Gibbs RJ (1970) Mechanisms controlling world water chemistry. J Sci 17:1088–1090

Guey-Shin S, Bai-You C, Chi-Ting C, Pei-Hsuan Y, TsunKuo C (2011) Applying factor analysis combined with kriging and information entropy theory for mapping and evaluating the stability of groundwater quality variation in Taiwan. Int J Environ Res Public Health 8:1084–1109

Guo H, Wang Y (2004) Hydrogeochemical processes in shallow quaternary aquifers from the northern part of the Datong Basin, China; Appl. Geochem 19(1):19–27

Jalali M (2005a) Nitrates leaching from agricultural land in Hamedan, western Iran. Agric Ecosyst Environ 110:210–218

Jalali M (2007) Salinization of groundwater in arid and semiarid zones: an example from tajarak, Western Iran. Environ Geol 52:1133–1149

Jalali M (2009) Groundwater geochemistry in the Alisadr, Hamadan, Western Iran. Nat Resour Res 21(1):61–73

Jalali M (2011) Hydrochemical characteristics and sodification of groundwater in the Shirin Sou, Hamadan, Western Iran. Nat Resour Res 21(1):61–73

Kalantary N, Rahmani M, Charchi A (2007) Use of composite diagram, factor analyses and saturation index for quantification of Zaviercherry and Kheran plain groundwaters. J Eng Geol 2(1):339–356

Karanth KR (1987) Groundwater assessment, development and management. Tata-McGraw-Hill, New Delhi

Kazemi GA, Mohammadi A (2012) Significance of hydrogeochemical analysis in the management of groundwater resources: a case study in northeastern Iran. Hydrogeology—a global perspective, Dr. Gholam A. Kazemi (Ed.), ISBN: 978–953-51-0048-5.

Li P, Qian H, Wu J, Chen J, Zhang Y, Zhang H (2013c) Occurrence and hydrogeochemistry of fluoride in shallow alluvial aquifer of Weihe River, China. Environ Earth Sci 71(7):3133–3145. doi:10.1007/s12665-013-2691-6

Li P, Qian H, Wu J, Ding J (2010) Geochemical modeling of groundwater in southern plain area of Pengyang County, Ningxia, China. Water Sci Eng 3(3):282–291. doi:10.3882/j.issn.1674-2370.2010.03.004

Li P, Qian H, Wu J, Zhang Y, Zhang H (2013a) Major ion chemistry of shallow groundwater in the Dongsheng Coalfield, Ordos Basin, China. Mine Water Environ 32(3):195–206. doi:10.1007/s10230-013-0234-8

Li P, Wu J, Qian H (2013b) Assessment of groundwater quality for irrigation purposes and identification of hydrogeochemical evolution mechanisms in Pengyang County, China. Environ Earth Sci 69(7): 2211–2225. doi:10.1007/s12665-012-2049-5

Li P, Wu J, Qian H (2014) Hydrogeochemistry and quality assessment of shallow groundwater in the Southern Part of the Yellow River alluvial plain (Zhongwei Section), China. Earth Sci Res J 18(1):27–38

Mahdavi M (2007) Applied hydrology. Tehran University Publication, Iran(In Persian)

McLean W, Jankowski J, Lavitt N (2000) Groundwater quality and sustainability in an alluvial aquifer, Australia. In: Sililo O et al. (eds) Groundwater, past achievements and future challenges. A Balkema, Rotterdam, pp. 567–573

Parkhurst DL, Appelo CAJ (1999) User's guide to PHREEQC (version 2), a computer program for speciation, batch-reaction, one-dimensional transport and inverse geochemical calculations. US Geological Survey, Water-Resources Investigations Report 99-4259.

Rademacher LK, Clark JF, Hudson GB, Erman DC, Erman NA (2001) Chemical evolution of shallow groundwater as recorded by springs, Sagehen basin. Nevada County. Calif Chem Geol 179:37–51

Rajmohan N, Elango L (2004) Identification and evolution of hydrogeochemical processes in an area of the Palar and Cheyyar River Basin, Southern India. Environ Geol 46:47–61

Richards LA (1954) Diagnosis and improvement of saline and alkaline soils. US Department of Agriculture, Washington, DC

Salama RB (1993) The chemical evolution of groundwater in a first-order catchment and the process of salt accumulation in the soil profile. J Hydrol 143:233–258

Saleh Al-Amry A (2008) Hydrogeochemistry and groundwater quality assessment in an arid region: a case study from Al Salameh Area, Shabwah, Yemen. The 3rd International Conference on Water Resources and Arid Environments and the 1st Arab Water Forum.

Sarath Prasanth SV, Magesh NS, Jitheshlal KV, Chandrasekar N, Gangadhar K (2012) Evaluation of groundwater quality and its suitability for drinking and agricultural use in the coastal stretch of Alappuzha District, Kerala, India. Appl Water Sci 2:165–175

Sikdar PK, Sarkar SS, Palchoudhury S (2001) Geochemical evolution of groundwater in the quaternary aquifer of Calcutta and Howrah. India J Asian Earth Sci 19:579–594

Sung KY, Yun ST, Park ME, Koh YK, Choi BY, Hutcheon I, Kim KH (2012) Reaction path modeling of hydrogeochemical evolution of groundwater in granitic bedrocks, South Korea. J Geochem Explor 118:90–97

Todd DK (1980) Groundwater hydrology [M], 2nd edn. Wiley, New York, p. 535

Van Wirdum G (1980) Description of water-quality changes in a hydrological cycle, for the purpose of nature conservation (in Dutch). In Waterquality in groundwater-flow systems, J.C. Hooghart (ed.), Commission for Hydrological Research TNO, The Hague, The Netherlands, Reports and notes 5, pp. 118–143.

Wang Y, Jiao JJ (2012) Origin of groundwater salinity and hydrogeochemical processes in the confined Quaternary aquifer of the Pearl River Delta, China. J Hydrol 438-439:112–124. doi:10.1016/j.jhydrol.2012.03.008

WHO (2004) Guidelines for drinking water quality. World Health Organization, Geneva

Wilcox LV (1958) The quality of water for irrigation. US Department of Agriculture.

World Health Organization (WHO) (2011) Guidelines for drinking-water quality, 4th Edn http://whqlibdoc.who.int/publications/2011/9789241548151_eng.pdf. Accessed 24 Nov 2012.

Wu J, Li P, Qian H, Duan Z, Zhang X (2014) Using correlation and multivariate statistical analysis to identify hydrogeochemical processes affecting the major ion chemistry of waters: case study in Laoheba phosphorite mine in Sichuan, China. Arab J Geosci 7(10):3973–3982. doi:10.1007/s12517-013-1057-4